Exploring the Design Space of 3_{10}-helical Bundles using Non-canonical Amino Acid

Xiyue Leng[1], Jonathan Clayden[1], and Derek N. Woolfson[1,2,3,4]

[1]School of Chemistry, [2]School of Biochemistry, and [3]Max Plack-Bristol Centre for Minimal Biology, University of Bristol, Bristol, UK; [4]Novo Nordisk Foundation Center for Protein Design, Department of Biology and Department of Drug Design and Pharmacology, University of Copenhagen, DK. 10.17952/38EPS.2026.P464 Presenting author: xiyue.leng@bristol.ac.uk

Overview Peptides and proteins based on α-amino acids predominantly adopt α-helical and β-strand structures, while extended assemblies of the noncanonical 3_{10} helix remain rare. We previously designed the *de novo* peptide $(\mathtt{ELUULK})_4$, which forms a hexameric 3_{10}-helical bundle in which Aib promotes 3_{10}-helix formation, Leu forms the hydrophobic core, and Glu/Lys define the solvent-exposed surface.[1] Here, we investigate the sequence requirements underlying this noncanonical fold and explore routes to its functionalisation. Surface substitutions are well tolerated, whereas the Aib flanking positions show substantially greater constraints. Core positions are more restrictive, with Leu uniquely supporting bundle formation among proteinogenic hydrophobic residues. Extending to seven hexad repeats enables substitution of two central core Leu residues with Ala or Gly while retaining stable, hexameric 3_{10}-helical assemblies. These substitutions generate hydrophobic cavities capable of binding environment-sensitive dyes. Together, these results define sequence constraints governing the stability of *de novo* 3_{10}-helical bundles and demonstrate how controlled core modification can alter these otherwise highly constrained assemblies.

1. Why design 3_{10} helices?

Extended 3_{10} helices occupy a narrow backbone-conformational region, and are rare as stand-alone higher-order assemblies in Nature.

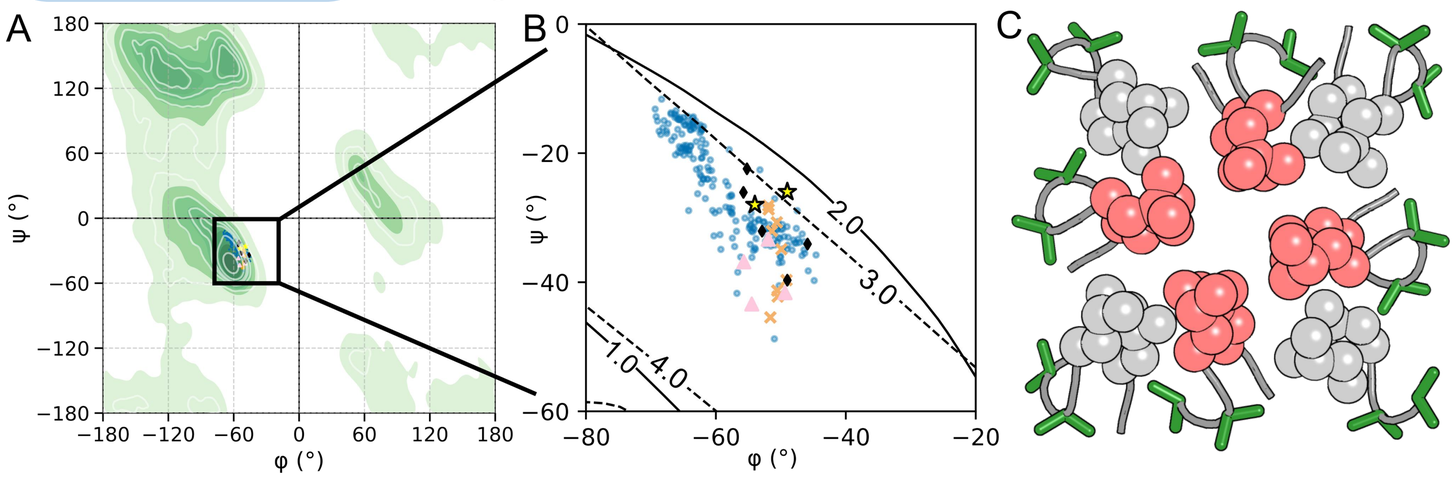


Fig. 1 Backbone geometry and design rationale of the 3_{10}-helical bundle. (**A**) Ramachandran distribution for residues in the Top8000 dataset overlayed with backbone dihedral angles (φ, ψ) from the representative 3_{10} helices extracted using the AMPAL library.[2-3] The experimental 3_{10} points occupy a restricted region adjacent to the α-helical basin; the green contour represents structural occurrence. (**B**) Expanded view of the region where φ is within (-80, -20) and ψ is within (-60,0) overlaid with helix parameters, rise per residue (Å) (solid line) and residues per turn (dotted line). The idealised 3_{10} helical geometry (3 residues per turn and 2.0 Å rise per residue) defines a narrow ridge, sampled by the experimental structures. (C) Top view of the X-ray crystal structure of *de novo* 3_{10}-helical bundle (PDB ID: 7qdi). The hydrophobic seam consisting of Leu side chains shown as spheres, featuring an inner (pink) and outer (grey) ring of helices.

2. A positional hierarchy of mutability

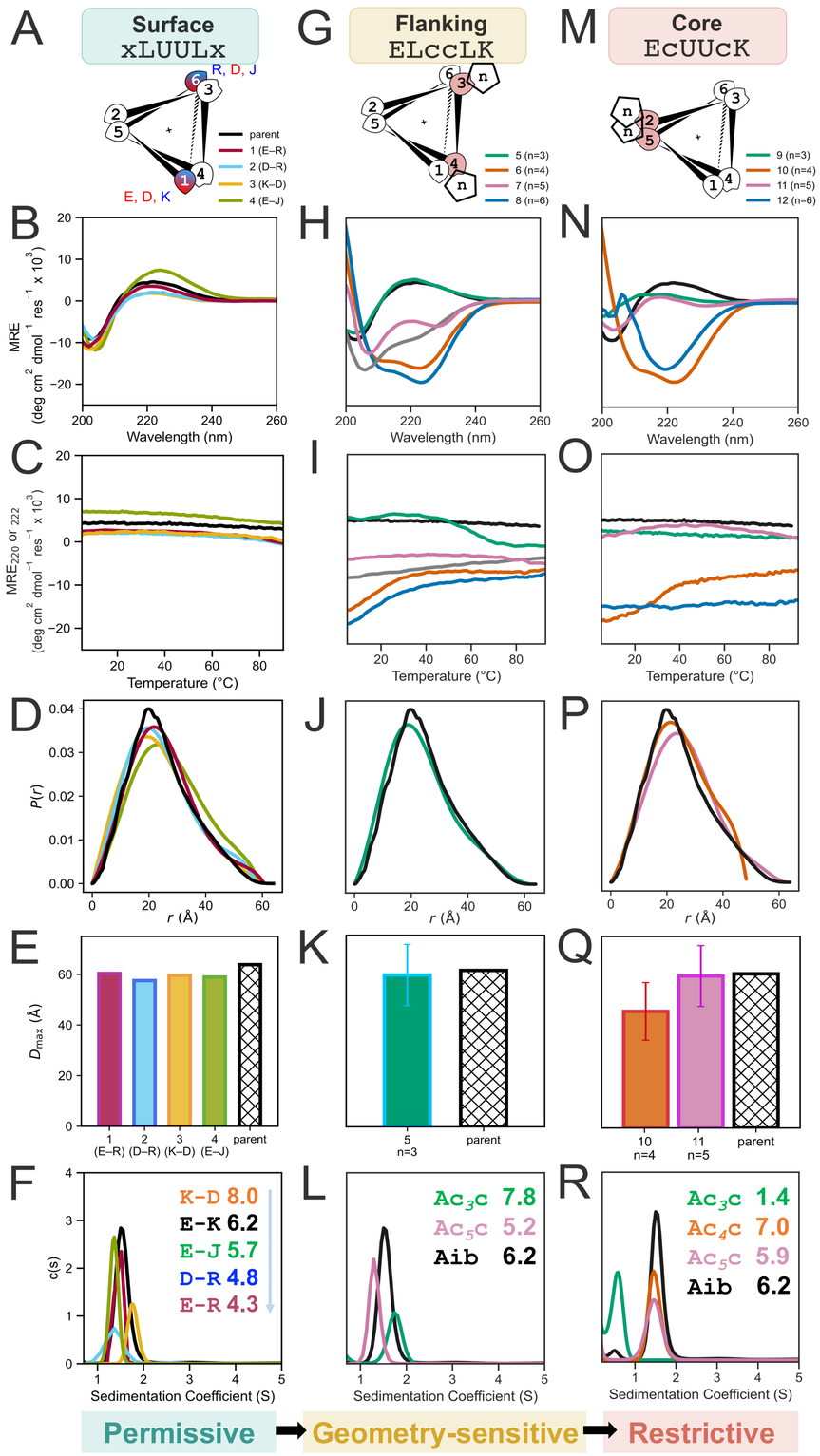


Fig. 2 Biophysical characterisation of surface (**1–4**), flanking (**5–8**), and core (**9–12**) variants, with the parent 3_{10}HD peptide as reference. (**A,G,M**) Helical-wheel representations and sequence motifs highlighting the substituted positions. (**B,H,N**) CD spectra at 5 °C. (**C,I,O**) Thermal unfolding monitored by CD at 220 or 222 nm (5–95 °C, 1 °C min⁻¹). (**D,J,P**) SAXS P(r) distributions and (**E,K,Q**) corresponding maximum particle dimensions. (**F,L,R**) Sedimentation-velocity AUC profiles showing the oligomeric states adopted in solution.

3. Residue energetics explain α ↔ 3_{10} switching

Dipeptide torsional free-energy surfaces provide residue-level context for the experimental switches.

Ac_3c shows the smallest energetic separation between α- and 3_{10}-helical basins, consistent with its greater compatibility with the noncanonical fold.

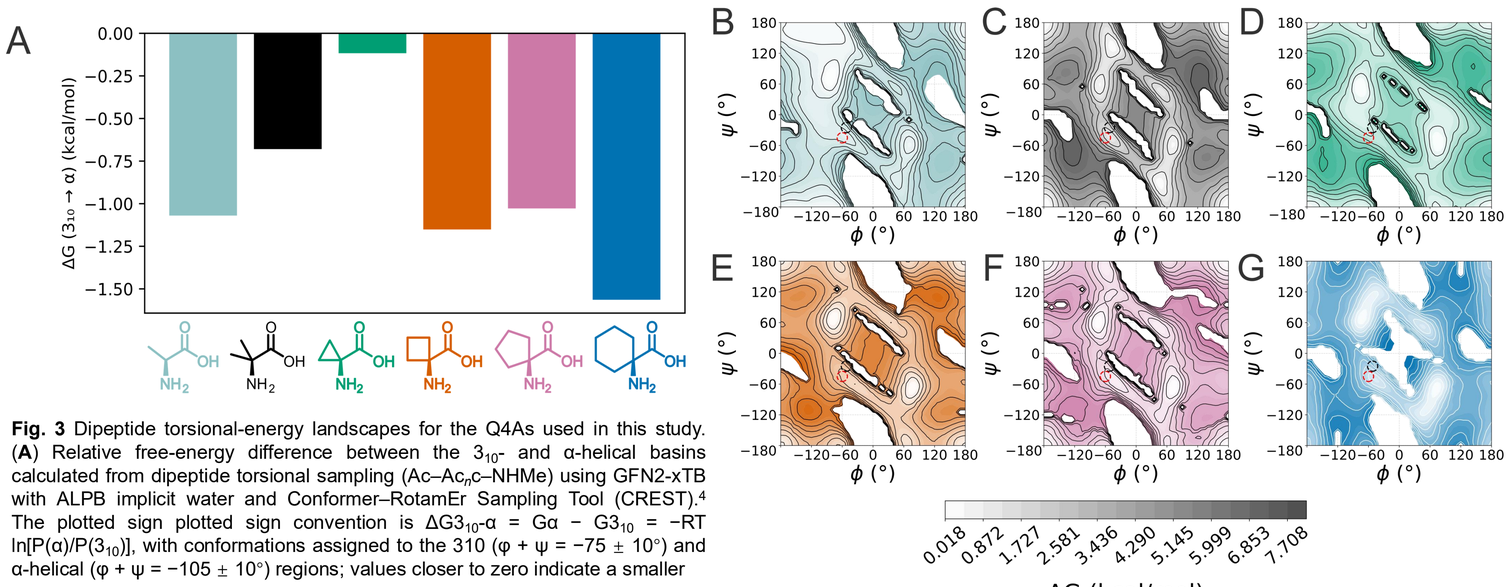


Fig. 3 Dipeptide torsional-energy landscapes for the Q4As used in this study. (**A**) Relative free-energy difference between the 3_{10}- and α-helical basins calculated from dipeptide torsional sampling (Ac–Ac_nc–NHMe) using GFN2-xTB with ALPB implicit water and Conformer–RotamEr Sampling Tool (CREST).[4] The plotted sign plotted sign convention is $\Delta G3_{10}$-α = Gα − $G3_{10}$ = −RT ln[P(α)/P(3_{10})], with conformations assigned to the 310 (φ + ψ = −75 ± 10°) and α-helical (φ + ψ = −105 ± 10°) regions; values closer to zero indicate a smaller energetic preference for α over 3_{10}. (**B–G**) Ramachandran free-energy distributions of Ala, Aib, and the larger cyclic Q4As show pronounced low-energy minima in the α-helical region, whereas Ac_3c gives the smallest separation between the two helical basins.

4. First demonstration of a functional 3_{10}-assembly

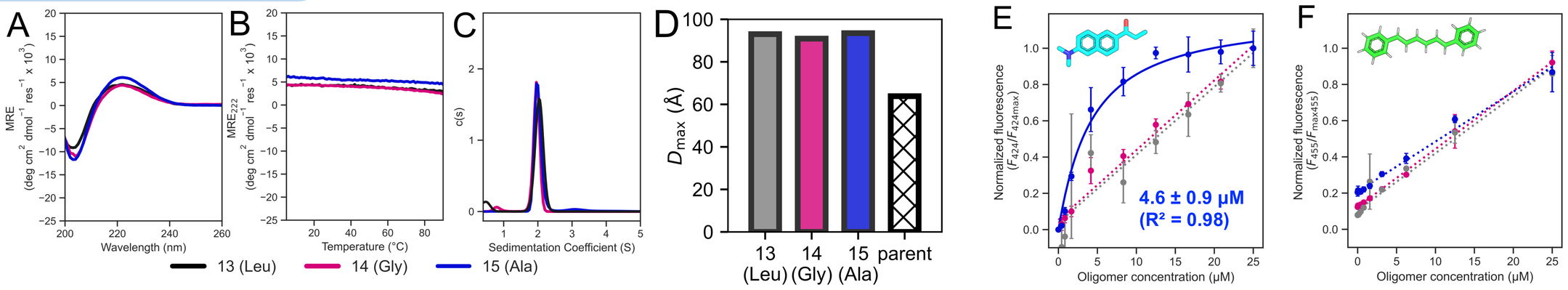


Fig. 4 Ligand recognition within extended 3_{10}-helical peptide assemblies **13–15**. Environment-sensitive dyes, 6-propionyl-2-dimethylaminonaphthalene (prodan) and 1,6-diphenylhexa-1.3,5-triene (DPH), have been assayed by us and others to probe for channels and cavities in *de novo* designed α-helical bundles and barrels.[5] Fluorescence-based binding assays only showed saturation binding for **15** with prodan, giving a dissociation constant (K_d) of 4.6 ± 0.9 μM (R^2 = 0.98). No saturation was observed for DPH binding under these conditions. Measurements were performed over 0–30 μM peptide oligomer with 1 μM dye in the final sample (5% v/v DMSO) at pH 7.4, upon incubation at 20 °C. Each dataset was normalised to its observed maximum fluorescence, and error bars represent the standard deviation of four replicate measurements.

Discussion and Conclusion The $(\mathtt{ELUULK})_4$ 3_{10}-helical bundle displays strongly position-dependent mutational tolerance. Surface residues can be readily substituted while preserving the 3_{10} architecture, whereas the interfacial Aib positions and hydrophobic core impose much tighter geometric constraints. Computational analysis indicates that successful 3_{10}-bundle formation requires both compatible backbone conformational preferences and precise side-chain geometry, explaining why small changes can redirect folding towards α-helical conformations or disrupt assembly entirely. Despite these constraints, extending the scaffold to seven hexad repeats enables controlled modification of the central hydrophobic core. Substitution of two Leu residues with Ala or Gly generates stable hexameric 3_{10}-helical bundles containing hydrophobic cavities that bind small environment-sensitive dyes in the μM range. This demonstrates that sequence extension can overcome local packing constraints and provides a route to functionalising 3_{10}-helical scaffolds through selective removal of methylene groups. Together, these results establish a sequence–structure framework for *de novo* 3_{10}-helical bundle design and show that, although more constrained than canonical α-helical assemblies, 3_{10} helices can serve as programmable scaffolds for tuning oligomerisation and creating defined molecular-recognition sites.

References

(1) Kumar, P.; Paterson, N. G.; Clayden, J.; Woolfson, D. N. *Nature* 2022, 607 (7918), 387–392. DOI: 10.1038/s41586-022-04868-x. (2) Hintze, B. J.; Lewis, S. M.; Richardson, J. S.; Richardson, D. C. *Proteins* 2016, 84 (9), 1177–1189. DOI: 10.1002/prot.25039. (3) Wood, C. W.; Heal, J. W.; Thomson, A. R.; Bartlett, G. J.; Ibarra, A. Å.; Brady, R. L.; Sessions, R. B.; Woolfson, D. N. *Bioinformatics* 2017, 33 (19), 3043–3050. DOI: 10.1093/bioinformatics/btx352 (acccessed 2024-08-08T13:56:36). (4) Pracht, P.; Grimme, S.; Bannwarth, C.; Bohle, F.; Ehlert, S.; Feldmann, G.; Gorges, J.; Müller, M.; Neudecker, T.; Plett, C.; et al. *J. Chem. Phys.* 2024, 160 (11). DOI: 10.1063/5.0197592 (5) Thomas, F.; Dawson, W. M.; Lang, E. J. M.; Burton, A. J.; Bartlett, G. J.; Rhys, G. G.; Mulholland, A. J.; Woolfson, D. N. *ACS Synth. Biol.* **2018**, 7 (7), 1808–1816. DOI: 10.1021/acssynbio.8b00225.